

A seasonality trigger for carbon injection at the Paleocene-Eocene thermal maximum

Published by Copernicus Publications on behalf of the European Geosciences Union.

Abstract

1 Introduction

5838

of such sources (Sluijs et al., 2007; Panchuk et al., 2008). At least 4 transient global warming events related to massive carbon input occurred through the late Paleocene – early Eocene, apparently paced by orbital cycles within the Milankovitch band (Lourens et al., 2005; Galeotti et al., 2010). Recent studies have therefore preferred mechanisms that require a climatological trigger for carbon injection, for example through enhancement of seasonal extremes that caused changes in ocean circulation, which in turn could dissociate submarine methane hydrates (Lunt et al., 2011).

Critically, several records suggest that some of the warming preceded the injection of ^{13}C -depleted carbon by several thousands of years, which may have triggered the injection of carbon (Sluijs et al., 2007; Secord et al., 2010). However, no data exist to evaluate if this warming included a seasonal bias. Such small time lags can only be resolved in stratigraphically expanded sediment sections, typically from marginal marine areas because deep-marine sections are condensed due to the massive dissolution of carbonates (Zachos et al., 2005). The Central North Sea basin yields vastly expanded PETM sections because of massive sediment supply from the hinterland (Sluijs et al., 2007). Numerous of such successions have been retrieved by oil exploration and production companies, but generally have not been made publically available. We studied Shell Exploration and Production well 22/11-N1 (57°39.46' N, 1°8.444' E, present water depth ~83 m) in the Central North Sea (Fig. 1). This core was drilled in 1991 from the Nelson Field platform penetrating the heterolithic sands and mudstones of the Forties fan system.

2 Results and discussion

The sediments in core 22/11-N1 are barren of calcareous and siliceous microfossils, but yield rich and abundant palynological assemblages, notably organic-walled dinoflagellate cysts (dinocysts; Fig. S2) and spores and pollen from higher plants (Fig. 2), suitable for paleoecological and paleoclimatological analyses. Along with palynological

5839

data, we generated high-resolution records of stable carbon isotope ratios ($\delta^{13}\text{C}$) of total organic carbon (TOC; Fig. 2).

2.1 $\delta^{13}\text{C}$ isotope data

A negative CIE of up to 3.8‰ occurs in $\delta^{13}\text{C}_{\text{TOC}}$ between 2264.5 and 2215.1 m below sea floor (mbsf; Fig. 2), followed by relatively stable values up to 2207.4 mbsf. This interval is also marked the abundant occurrence of the dinoflagellate *Apectodinium augustum* (Fig. S2), which is diagnostic of the PETM (Sluijs et al., 2007). This excludes the possibility that the CIE reflects one of the younger early Eocene transient global warming events (Lourens et al., 2005). However, the magnitude and shape of the CIE in well 22/11-N1 is anomalous compared to other records, which are usually characterized by an abrupt negative shift, often termed the “initiation”, followed by a phase of relatively stable, low values, which has been termed the “body” of the CIE, and a subsequent “recovery” to higher $\delta^{13}\text{C}$ values (McInerney and Wing, 2011). Our $\delta^{13}\text{C}_{\text{TOC}}$ record gradually declines by ~1‰ for the majority of the cored section, and shows a second decline of ~3‰ between 2224.4 and 2217.3 mbsf. The shape and magnitude of the record is likely impacted by changing contributions of various types of organic matter (Crouch et al., 2003). However, minimum $\delta^{13}\text{C}_{\text{TOC}}$ values are reached only ~50 m above the onset of the CIE, suggesting a massively expanded CIE. While the initiation of the CIE seems complete, our stratigraphic interpretation of the cored sediments from well 22/11-N1 (see Supplement) indicates an erosive surface at the base coarse sand unit (2225.2 mbsf), so that part of the “CIE body” is missing from the record. Furthermore, the “CIE recovery” phase in these sediments is relatively condensed, though could be part eroded, resulting in an incomplete record for this latter interval.

5840

2.2 Palynofloral assemblages

The terrestrial palynomorphs in well 22/11-N1 (Fig. 2) were mostly transported to the basin via submarine fans. However, the main trends are regionally defined, occurring both in shelf and pelagic sediments, and thus reflect regional climate events (see Supporting Information). Uppermost Paleocene sediments (2264.5–2285.1 mbsf) yield palynofloral assemblages dominated by the microthermal to mesothermal Pinaceae *Abies*, *Picea* and *Pinus*. Mesothermal conifers such as Taxodiaceae-Cupressaceae are also abundant, while dicots such as *Alnus* [alder], *Carya* [hickory], and *Juglans* [walnut] are consistently present. These taxa indicate the presence of a moderately diverse mixed conifer-broadleaf vegetation. Towards the PETM, an increase in mesothermal to megathermal taxa occurs including palms/cycads, *Engelhardtia* and Icacinaceae. The occurrence of palms/cycads indicates coldest month mean temperatures (CMMTs) > 5 °C in the modern (Greenwood and Wing, 1995). However, when grown under the high-CO₂ conditions that prevailed during the Eocene (Lowenstein and Demicco, 2006), palms are even less resilient to seasonal cooling, suggesting that CMMTs were > 8 °C (Royer et al., 2002). Hence, the first occurrence of palms/cycads at 2278.1 mbsf combined with increasing abundances of other megathermal taxa implies a shift to warmer climates.

The initiation of the CIE is characterized by an increase in ferns, namely Schizeaceae (cf. *Lygodium*, climbing fern) and Polypodiaceae (epiphytes), while palms/cycads, *Engelhardtia*, Icacinaceae are still represented. An abundance of ferns is generally associated with tropical to warm temperate wet climates, with the diversification of epiphytic ferns in the latest Paleocene-Eocene being associated with extreme warmth and the expansion of the topical forest biome to more mid-high latitudes (Schuttpelz and Pyrer, 2009; Harding et al., 2011). Within the CIE initiation interval, *Typha* spp./Sparganiaceae become an important component of the paleofloral assemblages, indicating an increase in the wetland component, represented by the development of rush/reed marshes in the coastal regions. This is consistent with the development of extensive

5841

wetlands in the North Sea region, and also the eastern US gulf coast during the CIE interval (Harrington, 2008).

The interval between 2225–2215 mbsf shows greater variability in the $\delta^{13}\text{C}_{\text{TOC}}$ signal, and is dominated by *Carya* spp., indicative of broadleaf forests and woodland communities. Palms/cycads are not present in this interval, which may support this interpretation. At ~2217 mbsf, a relatively sharp shift in paleoflora composition with a marked decrease in *Carya* spp. suggests possible condensation or an erosive surface (see Supplement). Above this interval, an increase in *Pinus* spp., *Alnus* and mesothermal elements such as Taxodiaceae-Cupressaceae and *Platycarya*, indicate the development of moderately diverse mixed conifer-broadleaf vegetation, potentially pointing to the recovery phase of the PETM. However, the presence of rare mesothermal-megathermal elements (e.g., palms/cycads, *Engelhardtia* and Icacinaceae) indicates the persistence of a relatively warm climate.

2.3 Bioclimatic analysis

We applied bioclimatic analysis, on the spore and pollen assemblages, a form of the Nearest Living Relatives (NLRs) method (see Supporting Information) to reconstruct mean annual temperature (MAT), CMMT and warm month mean temperature (WMMT) (Fig. 3). We assume that the ecological and climatic preferences of the fossil spore and pollen assemblages are similar to their extant living relatives.

2.3.1 Temperature reconstructions

Our data indicate that the late Paleocene climate was generally warm, with MAT ~ 14.5 ± 2.5 °C, CMMT > 6 °C and WMMT ~ 23 °C, respectively (Fig. 3b–d). Our data indicates that for the latest Paleocene, just prior to the CIE initiation, MAT is estimated at ~ 16 ± 2.5 °C, indicating a 1.5 °C warming, although it is also within the range limits of the data. However, of greatest significance are the estimates of WMMT, which are ~ 25.5 ± 1.1 °C, representing a 3 °C warming prior to the CIE. We also estimate

5842

CMMT at $\sim 9 \pm 2.2^\circ\text{C}$, indicating a less pronounced 2.5°C warming prior to the CIE. Our temperature estimates for MAT, WMMT and CMMT remain elevated throughout the CIE. Our data indicates that both CMMT and WMMT recover to pre- PETM values between 2218.1–2216.6 mbsf, however the carbon isotope stratigraphy suggests this interval remains within the CIE.

Comparison of our climate estimates for the Paleocene-Eocene boundary with other European records is difficult as there are no other climate estimates from Europe. Therefore, we compare to more distant records, where our estimates of MAT for the latest Paleocene are generally consistent with those estimates from leaf physiognomy from macrofloras from Bighorn Basin, which show an increase from $12.9 \pm 2.4^\circ\text{C}$ to over $15 \pm 2.4^\circ\text{C}$ (Wing and Harrington, 2002; Wing et al., 2005). For the PETM interval itself our estimates are generally somewhat lower than those recorded elsewhere, which estimate MAT between $20\text{--}26^\circ\text{C}$ based on oxygen isotopes of biogenic phosphate (Fricke et al., 1998), tooth enamel (Koch et al., 2003; Secord et al., 2010), soil nodules (Bowen et al., 2001); soil-derived bacterial membrane lipids (Weijers et al., 2007), and leaf margin analyses (Wing et al., 2005). This partly reflects the variable geographic locations of the selected records. However, these other records of MAT more closely resemble our WMMT estimates, though leaf physiognomy has been shown to yield cooler estimates than NLR-based approaches for the same fossil assemblage (Greenwood and Wing, 1995). The variation between our MAT estimate and those derived from oxygen isotope ratios of carbonate and phosphate components (tooth enamel; biogenic phosphate) could be due to seasonal bias in the oxygen isotope ratio of ingested water, while soil-derived bacterial membrane lipids could be biased towards summer values at high latitudes (Weijers et al., 2007). Alternatively, as our MAT estimates do not show a significant increase across the PETM it is possible that palynofloral composition and its geographic distribution are related less to mean annual temperatures but rather to seasonal differences, as demonstrated by significant temperature shifts in both CMMT and WMMT records.

5843

2.3.2 Precipitation reconstructions

We have also calculated precipitation estimates across the PETM of the North Sea, including mean annual precipitation (MAP), and the first seasonal precipitation estimates including cold month mean precipitation (CMMP) and warm month mean precipitation (WMMP). Estimates of MAP are high ($> 120 \text{ cm yr}^{-1}$), although there are large uncertainties in this estimate (Fig. 4b) they are similar to those estimated using leaf physiognomy from macrofloras from Wyoming, United States (Wing et al., 2005). However, we do not see a significant change in MAP, suggesting continued high precipitation and increased summer temperatures during the PETM, or insensitivity using our methodology to changes in MAP over the interval. Our estimates, however, are consistent with other evidence for high precipitation and continental runoff during the PETM (Schmitz and Pujalte, 2008; Sluijs et al., 2008). Despite the relatively large uncertainties in precipitation estimates, our seasonal precipitation record using WMMP and CMMP (Fig. 4c and d) does provide additional insights into the climate of PETM interval. In particular, our WMMP estimates (Fig. 4d) show a brief shift to wetter conditions pre-CIE, which although uncertainties are large coincides with the first common appearance of the freshwater algae *Pediastrum*. Our estimates also show a second more significant shift to higher summer precipitation ($\sim 140 \text{ cm yr}^{-1}$) late in the CIE initiation and into the CIE body. This latter shift in WMMP corresponds with an abundance of the freshwater peridinioid dinocyst taxon *Bosedinia* (Prauss, 2012) indicating enhanced continental runoff and salinity stratification in the central North Sea Basin at this time associated with the higher summer precipitation.

3 Conclusions

Our data indicates that there was a significant shift towards a seasonally warmer climate, in particular an increase in WMMT, greater in magnitude than the mean annual temperature changes. This climate shift is reflected in particular by (1) reductions in

5844

boreal conifers such as Pinaceae and (2) increase in mesothermal to megathermal taxa including palms/cycads, *Engelhardtia* and Icacinaceae. The change in vegetation we report occurs prior to the CIE. It is concomitant with the onset of the *Apectodinium* acme prior to the CIE in well 22/11-N1, representing the earliest sign of anomalous PETM-related environmental change also at other North Sea sites (Sluijs et al., 2007). Within the CIE, there is significant re-organization of the vegetation with initial increases in epiphytic and climbing ferns (Polypodiaceae and Schizeaceae), and development of extensive wetlands, followed by abundance of *Carya* spp., indicative of broadleaf forests. Our precipitation estimates although have large uncertainties provide the first direct evidence for seasonally wetter summers briefly prior to the CIE and more persistently during the main CIE itself. These shifts to wetter summers correspond with periods on enhanced continental runoff as expressed by the abundance of freshwater indicators such as the algae *Pediastrum* and the dinocyst taxon *Bosedinia* and are consistent with enhanced hydrological cycling prior to, and during the PETM interval.

The marked increase in WMMT and WMMP puts a new perspective on environmental precursors to the injection of carbon during the PETM. Previous studies found anomalous biotic change and at least regional warming to lead the CIE by thousands of years (Thomas et al., 2002; Sluijs et al., 2007; Secord et al., 2011). This suggested that early warming could have caused destabilization of submarine methane hydrates to cause injection of ^{13}C -depleted carbon into the global exogenic carbon pool. Recent experiments with a fully coupled atmosphere–ocean climate general circulation model (GCM) supported this scenario (Lunt et al., 2011). In this model, enhanced seasonal contrasts through milankovitch forcing (Lourens et al., 2005), combined with a gradually warming late-Paleocene to early Eocene, forced a non-linear response in ocean circulation to warm intermediate waters. This mechanism, which explains not only the PETM but also the smaller early Eocene events, should have caused hydrate dissociation if these were present in the early Paleogene (Lunt et al., 2011). Our results show the occurrence of such seasonal extremes just prior to the onset of the CIE and may

5845

thus represent the smoking gun of a climatologically forced threshold in the carbon cycle that caused the PETM.

4 Materials and methods

4.1 Palynology

Samples were demineralised using cold hydrochloric (30 % HCl) and hydrofluoric (60 % HF) acids. Concentrated nitric acid (70 % HNO_3) was then employed for oxidation purposes, followed by sieving through ten-micron and thirty-micron sieves to concentrate the remaining residues, which were then air-dried on coverslips and mounted on slides using Elvacite. Residues were analysed using a stereo-binocular microscope until the entire slide was counted for terrestrial palynomorphs.

4.2 Bioclimatic analyses

Bioclimatic analysis derives estimates of temperature and precipitation parameters (i.e. MAT, CMMT, WMMT and MAP) based on the potential overlap of the climate range in the modern world of the identified nearest living relatives (NLRs) of the fossil spore and pollen found in a single sample. It differs from “threshold” methods, such as the presence of temperature sensitive taxa such as palms (Greenwood and Wing, 1995; Royer et al., 2002) by reconstructing the climate space that can accommodate a majority of the identified taxa’s NLRs. The bioclimatic method is outlined in the Supporting Information. Those taxa that were utilised in this study and their NLRs can be found in Supplement Table S1.

Supplementary material related to this article is available online at
<http://www.clim-past-discuss.net/9/5837/2013/cpd-9-5837-2013-supplement.zip>.

5846

Acknowledgements. We thank Arnold van Dijk for analytical support and Gert-Jan Reichart (Utrecht University) for discussions. DRG's research is supported by NSERC (Canada). AS thanks the European Research Council under the European Community's Seventh Framework Program for funding through ERC Starting Grant #259627. Author Contributions: J. S. Eldrett conducted palynological analyses; D. R. Greenwood carried out bioclimatic analyses; M. Polling conducted isotope analyses; J. S. Eldrett, D. R. Greenwood, H. Brinkhuis and A. Sluijs co-wrote the paper. The authors declare no conflict of interest. This article contains supporting information online at <http://www.climate-of-the-past.net/home.html>.

References

- 10 Bowen G. J., Koch, P. L., Gingerich, P. D., Norris, R. D., Bains, S., and Corfield, R. M.: Refined isotope stratigraphy across the continental Paleocene-Eocene boundary on Polecat Bench in the Northern Bighorn Basin, in: *Paleocene-Eocene Stratigraphy and Biotic Change in the Bighorn and Clarks Fork Basins, Wyoming*, edited by: Gingerich, P. D., Univ. of Michigan Papers on Palaeontology, 33, Ann Arbor, MI, 73–88, 2001.
- 15 Crouch, E. M., Dickens, G. R., Brinkhuis, H., Aubry, M.-P., Hollis, C. J., Rogers, K. M., and Vischer, H.: The Apectodinium acme and terrestrial discharge during the Paleocene-Eocene thermal maximum: new palynological, geochemical and calcareous nannoplankton observations at Tawanui, New Zealand, *Palaeogeogr. Palaeoclimatol.*, 194, 387–403, 2003.
- DeConto R. M., Galeotti, S., Pangani, M., Tracy, D., Schaefer, K., Tingjun, Z., Pollard, D., and Beerling, D. J.: Past extreme warming events linked to massive carbon release from thawing permafrost, *Nature*, 484, 87–91, 2012.
- 20 Dickens, G. R., O'Neil, J. R., Rea, D. K., and Owen, R. M.: Dissociation of oceanic methane hydrate as a cause of the carbon isotope excursion at the end of the Paleocene, *Palaeoceanography*, 23, 965–971, 1995.
- 25 Dickens, G. R., Castillo, M. M., and Walker, J. C. G.: A blast of gas in the latest Paleocene, simulating first order effects of massive dissociation of oceanic methane hydrate, *Geology*, 25, 259–262, 1997.
- Fricke, H. C., Clyde, W. C., O'Neil, J. R., and Gingerich, P. D.: Evidence for rapid climate change in North America during the latest Paleocene thermal maximum: oxygen isotope

5847

- compositions of biogenic phosphate from the Bighorn Basin (Wyoming), *Earth Planet. Sc. Lett.*, 160, 193–208, 1998.
- Galeotti, S., Krishnan, S., Pangani, M., Lanci, L., Gaudio, A., Zachos, J. C., Monechi, S., Morelli, G., and Lourens, L.: Orbital chronology of early Eocene hyperthermals from the Contessa Road section, central Italy, *Earth Planet. Sc. Lett.*, 290, 192–200, 2010.
- 5 Greenwood, D. R. and Wing, S. L.: Eocene continental climates and latitudinal temperature gradients, *Geology*, 23, 1044–1048, 1995.
- Harding, I. C., Charles, A. J., Marshall, J. E. A., Pälike, H., Roberts, A. P., Wilson, P. A., Jarvis, E., Thorne, R., Morris, E., Moremon, R., Pearce, R. B., and Akbari, S.: Sea-level and salinity fluctuations during the Paleocene-Eocene thermal maximum in Arctic Spitsbergen, *Earth Planet. Sc. Lett.*, 258, 581–592, 2011.
- 10 Harrington, G. J.: Comparisons between Paleocene-Eocene paratropical swamp and marginal marine pollen floras from Alabama and Mississippi, USA, *Palaeontology*, 51, 611–622, 2008.
- Koch, P. L., Cylde, W. C., Hepple, R. P., Fogel, M. L., Wing, S. L., and Zachos, J. C.: Carbon and oxygen isotope records from paleosols spanning the Paleocene-Eocene boundary, Bighorn Basin, Wyoming, in: *Causes and Consequences of Globally Warm Climates in the Early Palaeogene*, edited by: Wing, S. L., Gingerich, P. D., Schmitz, B., and Thomas, E., Geological Society of America Special Paper, 369, 49–64, 2003.
- 15 Kurtz, A. C., Kump, L. R., Arthur, M. A., Zachos, J. C., and Paytan, A.: Early Cenozoic decoupling of the global carbon and sulphur cycles, *Palaeoceanography*, 18, 1090–1104, 2003.
- 20 Lourens, L. J., Sluijs, A. P., Kroon, D., Zachos, J. C., Thomas, E., Röhl, U., Bowles, J., and Raffi, I.: Astronomical pacing of late Palaeocene to early Eocene global warming events, *Nature*, 435, 1083–1087, 2005.
- Lowenstein, T. K. and Demicco, R. V.: Elevated Eocene atmospheric CO₂ and its subsequent decline, *Science*, 313, 1928, doi:10.1126/science.1129555, 2006.
- 25 Lunt, D. J., Ridgwell, A., Sluijs, A., Zachos, J. C., Hunter, S., and Haywood, A.: A model for orbital pacing of methane hydrate destabilization during the Palaeogene, *Nat. Geosci.*, 4, 775–778, 2011.
- McInerney, F. A. and Wing, S. L.: The Paleocene-Eocene thermal maximum: a perturbation of the carbon cycle, climate, and biosphere with implications for the future, *Earth Planet. Sc. Lett.*, 39, 489–516, 2011.
- 30 Panchuk, K., Ridgwell, A., and Kump, L. R.: Sedimentary response to Paleocene-Eocene Thermal Maximum carbon release: a model-data comparison, *Geology*, 36, 315–318, 2008.

5848

- Prauss, M. L.: The Cenomanian/Turonian Boundary event (CTBE) at Tarfaya, Morocco: palaeoecological aspects as reflected by marine palynology, *Cretaceous Res.*, 34, 233–256, 2012.
- Royer, D. L., Osborne, C. P., and Beerling, D. J.: High CO₂ increases the freezing sensitivity of plants: implications for palaeoclimatic reconstructions from fossil floras, *Geology*, 30, 963–966, 2002.
- Schuettpelz, E. and Pryer, K. M.: Evidence for a Cenozoic radiation of ferns in an angiosperm-dominated canopy, *P. Natl. Acad. Sci. USA*, 106, 11200–11205, doi:10.1073/pnas.0811136106, 2009.
- Secord, R., Gingerich, P. D., Lohmann, K. C., and MacLeod, K. G.: Continental warming preceding the Palaeocene-Eocene thermal maximum, *Nature*, 467, 955–958, 2010.
- Schmitz, B. and Pujalte, V.: Abrupt increase in seasonal extreme precipitation at the Paleocene-Eocene boundary, *Geology*, 35, 215–218, 2007.
- Sluijs, A., Brinkhuis, H., Schouten, S., Boharty, S. M., John, C. M., Zachos, J. C., Reichart, G.-J., Sinninghe Damsté, J. S., Crouch, E. M., and Dickens, G. R.: Environmental precursors to rapid light carbon injection at the Palaeocene/Eocene boundary, *Nature*, 450, 1218–1221, 2007.
- Sluijs, A., Brinkhuis, H., Crouch, E. M., John, C. M., Handley, L., Munsterman, D., Boharty, S. M., Zachos, J. C., Reichart, G.-J., Schouten, S., Pancost, R. D., Sinninghe Damsté, J. S., Welters, N. L. D., Lotter, A. F., and Dickens, G. R.: Eustatic variations during the Paleocene-Eocene greenhouse world, *Palaeoceanography*, 23, PA4216, doi:10.1029/2008PA001615, 2008.
- Svensen, H., Planke, S., and Corfu, F.: Zircon dating ties NE Atlantic sill emplacement to initial Eocene global warming, *J. Geol. Soc. London*, 167, 433–436, 2010.
- Thomas, D. J., Zachos, J. C., Bralower, T. J., Thomas, E., and Boharty, S.: Warming the fuel for the fire: evidence for the thermal dissociation of methane hydrate during the Paleocene-Eocene thermal maximum, *Geology*, 30, 1067–1070, 2002.
- Weijers, J. W. H., Schouten, S., Sluijs, A., Brinkhuis, A., and Sinninghe Damsté, J. S.: Warm arctic continents during the Palaeocene-Eocene thermal maximum, *Earth Planet. Sc. Lett.*, 261, 230–238, 2007.
- Wing, S. L. and Harrington, G. J.: Floral response to rapid warming in the earliest Eocene and implications for concurrent faunal change, *Palaeobiology*, 27, 539–563, 2001.

5849

- Wing, S. L., Harrington, G. J., Smith, F. A., Bloch, J. I., Boyer, D. M., and Freeman, K. H.: Transient floral change and rapid global warming at the Paleocene-Eocene boundary, *Science*, 310, 993–996, 2005.
- Zachos, J. C., Röhl, U., Schellenberg, S. A., Sluijs, A., Hodell, D. A., Kelly, D. C., Thomas, E., Nicolo, M., Raffi, I., Lourens, L. J., McCarren, H., and Kroon, D.: Rapid acidification of the ocean during the Paleocene-Eocene Thermal Maximum, *Science*, 308, 1611–1615, 2005.

5850

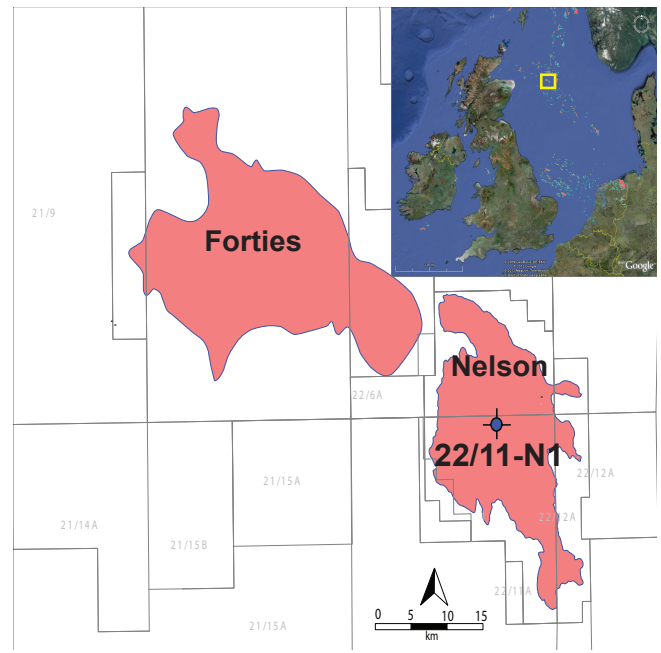


Fig. 1. Location map of well 22/11-N1, Nelson Field, Central North Sea (CNS). Coloured polygons representing oil and gas fields.

5851

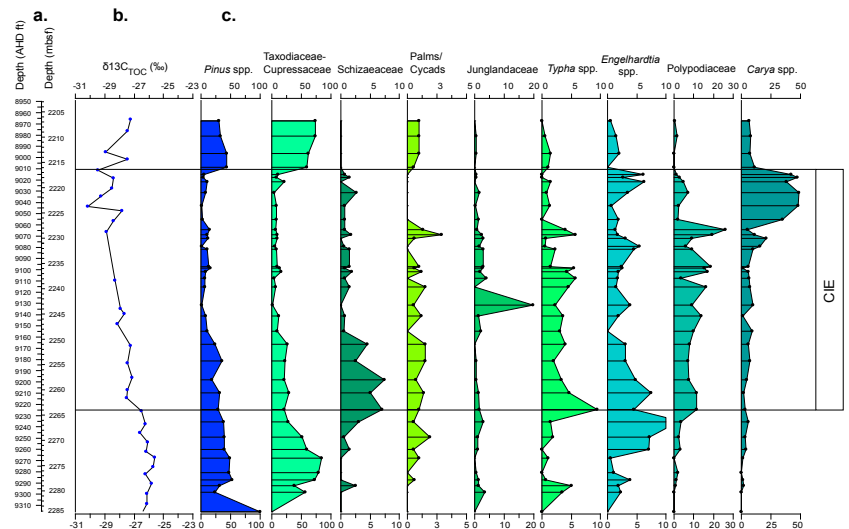


Fig. 2. Data from well 22/11-N1. (a) Carbon isotope data ($\delta^{13}\text{C}_{\text{TOC}}$), (b) selected spore and pollen percentage abundance.

5852

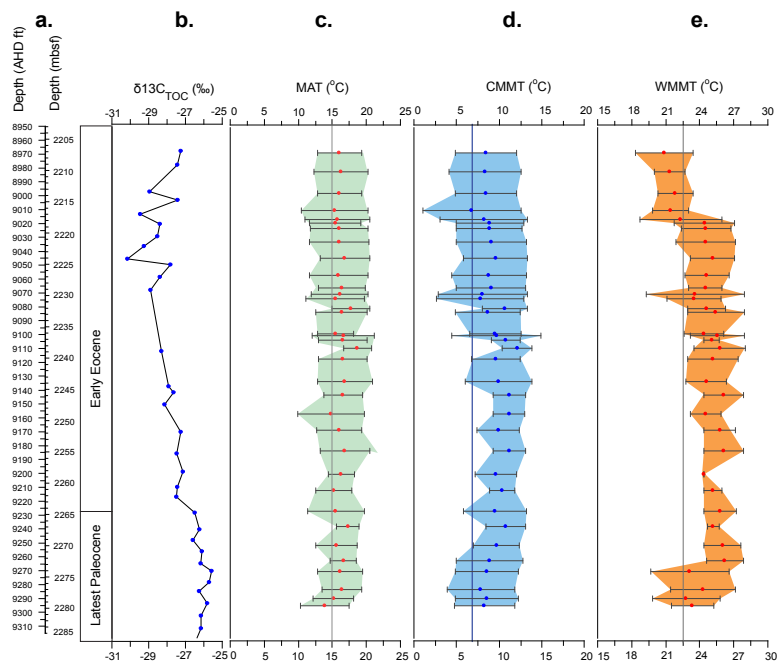


Fig. 3. Record of Paleocene-Eocene temperature data from well 22/11-N1. **(a)** Depth and age, **(b)** carbon isotope data ($\delta^{13}\text{C}_{\text{TOC}}$), **(c)** MAT; **(d)** CMMT; **(e)** WMMT. **(c–e)** Horizontal error bars and shaded area represent the minimum and maximum estimate returned from the method.

5853

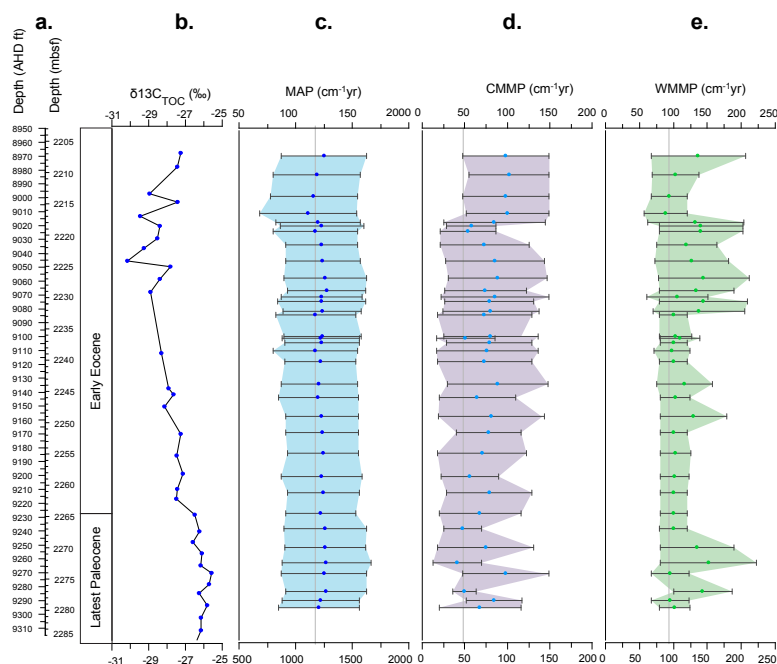


Fig. 4. Record of Paleocene-Eocene precipitation data from well 22/11-N1. **(a)** Depth and age, **(b)** carbon isotope data ($\delta^{13}\text{C}_{\text{TOC}}$), **(c)** MAP; **(d)** CMMP; **(e)** WMMP. **(c–e)** Horizontal error bars and shaded area represent the minimum and maximum estimate returned from the method.

5854